Energy & Environmental Science

Cite this: *Energy Environ. Sci.*, 2012, **5**, 9795

www.rsc.org/ees

PAPER

Morphological transformation during cross-linking of a highly sulfonated poly(phenylene sulfide nitrile) random copolymer†

So Young Lee,‡[a] Na Rae Kang,‡[b] Dong Won Shin,[a] Chang Hyun Lee,[d] Kwan-Soo Lee,[e] Michael D. Guiver,[bc] Nanwen Li[b] and Young Moo Lee*[ab]

Received 19th April 2012, Accepted 5th October 2012
DOI: 10.1039/c2ee21992a

We present a new approach of morphological transformation for effective proton transport within ionomers, even at partially hydrated states. Highly sulfonated poly(phenylene sulfide nitrile) (XESPSN) random network copolymers were synthesized as alternatives to state-of-the-art perfluorinated polymers such as Nafion®. A combination of thermal annealing and cross-linking, which was conducted at 250 °C by simple trimerisation of ethynyl groups at the chain termini, results in a morphological transformation. The resulting nanophase separation between the hydrophilic and hydrophobic domains forms well-connected hydrophilic nanochannels for dramatically enhanced proton conduction, even at partially hydrated conditions. For instance, the proton conductivity of XESPSN60 was 160% higher than that of Nafion® 212 at 80 °C and 50% relative humidity. The water uptake and dimensional swelling were also reduced and mechanical properties and oxidative stability were improved after three-dimensional network formation. The fuel cell performance of XESPSN membranes exhibited a significantly higher maximum power density than that of Nafion® 212 under partially hydrated environments.

Introduction

Polymer electrolyte fuel cells (PEFCs) are perceived as environmentally friendly energy conversion devices for both transportation and stationary power systems.[1] The polymer electrolyte membrane (PEM), which is a key component in determining PEFC performance, should satisfy tough criteria such as low production cost and physico-chemical durability.[2,3] Another important PEM requirement is fast proton conduction, even under either low relative humidity (RH) or elevated temperature (*e.g.*, the US Department of Energy (DOE) target is >0.1 S cm^{-1} at 80 °C and 50% RH),[4] enabling a simplified PEFC water management system design to reduce parasitic power losses.

[a]*School of Chemical Engineering, College of Engineering Hanyang University, Seoul 133-791, Republic of Korea. E-mail: ymlee@hanyang.ac.kr*
[b]*WCU Department of Energy Engineering, Hanyang University, Seoul 133-791, Republic of Korea*
[c]*National Research Council, Ottawa, Ont, KIA OR6, Canada*
[d]*Department of Green Energy Engineering, College of Engineering, Uiduk University, Gyeongju 780-713, Republic of Korea*
[e]*The 6th Research Team, Daedeok Research Institute, Honam Petrochemical Corp., Daejeon 305-726, Republic of Korea*
† Electronic supplementary information (ESI) available. See DOI: 10.1039/c2ee21992a
‡ These authors contributed equally to this work.

Broader context

A new thermal trimerisation of the terminal ethynyl groups in highly sulfonated poly(phenylene sulfide nitrile) (ESPSN) random network copolymers would morphologically transform the nanophase separation between hydrophilic and hydrophobic domains, leading to narrow and well-connected hydrophilic channels of diameter 15–20 nm. This unique morphologically transformed ESPSN network polymer leads to higher proton conduction capability than that of Nafion® 212 even at reduced relative humidity (30–50 RH%). Excellent physical and chemical stability coupled with dimensional stability were obtained *via* an end group cross-linking strategy and incorporation of sulfide groups into the polymer backbone. The rapid proton transport in water resulted from a synergetic effect of 3-D network formation-induced morphological transformation into well-connected hydrophilic–hydrophobic nanophase-separated domains and chain flexibility as demonstrated by high elongation values, in addition to its enhanced ionic concentration. A new network approach of the random copolymer makes it durable and an effective polymer electrolyte membrane material for automotive fuel cell applications, where an environment of elevated temperature and low humidity may exist.

To date, PEM materials with diverse chemical architectures and additives have been investigated as alternatives to perfluorinated sulfonic acid state-of-the-art ionomers such as Nafion®. The potential candidates are mainly derived from relatively cheap aromatic hydrocarbons, and are composed of hydrophilic and hydrophobic moieties for proton transport and mechanical integrity, respectively. The effective formation of well-connected water structures for rapid proton conduction has been achieved by the polymer architecture such as multiblock copolymers,[5–8] comb-shaped or triblock copolymers,[9–12] highly sulfonated copolymers,[13,14] and side-chain sulfonated polymers.[15] However, the proton conductivity is typically low under partially hydrated conditions.[16]

A promising strategy to overcome this barrier is to use highly sulfonated copolymers as proton conduction media and, simultaneously, to suppress excessive water swelling through cross-linking,[17] fabrication of organic–inorganic composites,[18–20] reinforcement structure formation,[21,22] or hydrophobic post-treatment.[23,24]

In the present study, self-cross-linkable disulfonated poly(phenylene sulfide nitrile) random copolymer (ESPSN) precursors were prepared *via* (1) polycondensation and subsequent nucleophilic substitution for the synthesis of starting random copolymers (SPSN) and (2) the incorporation of thermally curable ethynyl units at their termini, respectively. SPSN has a copolymer backbone derived from poly(phenylene sulfide nitrile), a high performance thermoplastic with high thermal and chemical stability, and with excellent electrical insulation properties and mechanical strength.[25–30] The sulfide (–S–) linkages are readily converted into sulfones (–SO_2–) upon exposure to H_2O_2, which is a by-product evolved at the cathode during PEFC operation and which forms free radicals associated with membrane degradation. The resulting –SO_2– linkages have superior stability toward radical attack[31] and also increase the acidity of sulfonic acid (–SO_3H) groups, owing to their strong electron-withdrawing property. Thus, the chemical transformation enables SPSN to have improved oxidative stability for extended PEM lifetime and to achieve high proton conductivity even at low humidity.[32] The nitrile (–C≡N) groups can give rise to strong dipolar inter-chain interactions with –SO_3H and/or other –C≡N groups in SPSN chains. The SPSN copolymer membrane is believed to be free from severe dimensional-change under a hydrated state[33] and to form a more stable interface with Nafion® electrodes.[34] Moreover, the thermally activated curing of the terminal ethynyl groups of ESPSN results in a firm three-dimensional (3-D) network, which is chemically stable even under challenging PEFC operating conditions.

Experimental section

Materials

4,4′-Dichlorodiphenyl sulfone (DCDPS), 4,4′-thiobisbenzene thiol (TBBT), 3-ethynylphenol, dimethylacetamide (DMAc) and toluene were purchased from Sigma Aldrich Co. (WI, USA). 2,6-Dichlorobenzonitrile (DCBN), decafluorobiphenyl (DFBP) and potassium carbonate (K_2CO_3) were purchased from TCI Co. (Tokyo, Japan). TBBT and DCBN were purified by recrystallization in dichloromethane and ethanol respectively before use. DCDPS was converted to 3,3′-disulfonate-4,4′-dichlorodiphenyl sulfone (SDCDPS) by using fuming sulfuric acid (40% SO_3, Sigma Aldrich, WI, USA), followed by neutralization with NaOH. SDCDPS and K_2CO_3 were used after vacuum drying at 120 °C for 1 day.

ESPSN synthesis

ESPSN copolymers were synthesized through sequential polycondensation and nucleophilic substitution. ESPSN60 is given as a representative example. TBBT (2.5041 g, 10 mmol), SDCDPS (3.0294 g, 6.1 mmol), DCBN (0.5676 g, 3.3 mmol), K_2CO_3 (2.0731 g, 15 mmol), DMAc (40 mL) and toluene (20 mL) were added into a 250 mL four-neck flask equipped with a mechanical stirrer, a Dean–Stark trap, a thermometer and a reflux condenser. After dehydration at 140 °C for 4 h and toluene removal, the solution mixture was heated up to 165 °C. The temperature was maintained at 165 °C for one day. Then, DFBP (0.4198 g, 0.3 mmol) solution in DMAc (10 mL) was added and stirred at 100 °C for 12 h. For incorporating ethynyl groups, 3-ethynylphenol (0.1380 g, 0.3 mmol) in a mixture of DMAc (10 mL) and toluene (10 mL) was added to DFBP-end-capped SPSN solution. After the reaction for 4 h, the resulting viscous polymer solution was precipitated from a mixture of isopropanol–water (70 : 30 by volumetric percentage). The residual salts were completely removed after hot water treatment repeatedly. ESPSN60 was dried under vacuum at 120 °C for 1 day. A series of ESPSN was prepared by controlling the ratio of SDCDPS to DCBN, using the same synthetic protocols.

Membrane fabrication and thermal curing

Prior to solution casting, each ESPSN solution in DMAc (15 wt%) was filtered with a 0.45 μm PTFE syringe filter and degassed under vacuum. The ESPSN solution cast on a clean glass plate was dried at 45 °C for 1 day, 60 °C for 2 h and 120 °C for 1 day for the membrane formation. For thermally cured XESPSN preparation, additional thermal treatment was performed in an oven at 250 °C for 100 min. The resulting potassium salt form of XESPSN membranes was acidified by treating in 1 M boiling H_2SO_4 solution for 4 h and boiling water for another 4 h. The thickness of the membrane was ~60 μm.

Characterization

The structural analysis of cross-linkable ESPSN was performed using ^{1}H NMR spectra (VNMRS600, Bruker, Germany) with d_6-dimethylsulfoxide (d_6-DMSO) as a solvent. The molecular weights of ESPSN were determined by gel permeation chromatography (GPC) with two Styragel® columns and a Waters2414 refractive index detector with *N*-methyl-2-pyrrolidone (NMP) containing 0.05 M LiBr as an eluent. Molecular weight was calibrated with a poly(methyl methacrylate) standard.

Differential scanning calorimetry (DSC, Q20, TA Instruments, USA) was used for determining thermal properties and the cross-linking temperature of ESPSN. Prior to the thermal analysis, ESPSN60 solution cast on the glass plate was dried at 45 °C for 1 day, 60 °C for 2 h and then 120 °C for 1 day to make a ESPSN60 film. The film was carefully peeled off from the glass and installed into a DSC pan. DSC measurements were conducted three times in the temperature range from 30 °C to 300 °C

with a heat flow rate of 10 °C min^{-1}. In addition, the degree of crosslinking at various curing temperatures of ESPSN was observed by DSC. Curing temperatures of 200 °C, 220 °C and 250 °C were selected and the heat flow was observed by isothermal curing temperature for the cross-linking reaction. The heating rate was 10 °C min^{-1}. The degree of cross-linking was calculated as $y = (H_t/H_T) \times 100$, where H_t is the total heat flow of sample mass for a given cross-linking time t and H_T is the total heat flow of sample mass for a cross-linking time of 100 min.

The membrane density was measured after acidification. Before measurement, the membranes were dried in a vacuum oven at 120 °C and isooctane (density = 0.693 g cm^{-3}) was used as the measurement solvent.

For transmission electron microscopy (TEM) and TEM-selected area diffraction (SAD) pattern observations, the membranes were stained with lead ions by ion exchange of the sulfonic acid groups in 0.5 M lead acetate aqueous solution. To avoid precipitation as well as the oxidation of lead ions, the membranes were stained for a short time in a glove box and rinsed repeatedly with deionized water, and then dried in a vacuum oven for 12 h. The stained membranes were embedded in epoxy resin, sectioned to 80 nm in thickness with a RMC MTX Ultra microtome, and placed on copper grids. Images were taken with a Carl Zeiss LIBRA 120 energy-filtering transmission electron microscope at an accelerating voltage of 120 kV.

Water uptake (WU) and dimensional change were determined by measuring the weight, area and thickness of membranes in the acid form, before and after hydration. Initial measurements were made after the membranes were dried under vacuum at 120 °C for 12 h. Then the membranes were immersed in deionized water and stirred for one day to reach equilibrium at given temperatures (30 °C and 80 °C). Before weight measurements of the hydrated membranes, the surface water was removed. Weight-based water uptake (WU_w) and volumetric water uptake (WU_v) were calculated with the following equations. Volumetric water uptake (WU_v) was determined from the density of water (δ_w) and the dried membrane (δ_m).

$$WU_w(wt\%) = \frac{W_{wet} - W_{dry}}{W_{dry}} \times 100 \quad (1)$$

$$WU_v(vol\%) = \frac{(W_{wet} - W_{dry})/\delta_w}{(W_{dry}/\delta_w)} \times 100 \quad (2)$$

where W_{dry} and W_{wet} are the weights of dried and wet membranes, respectively.

Dimensional swelling of membranes was determined by measuring area (in-plane swelling) and thickness (through-plane swelling) changes in the samples after they were initially dried at 120 °C for 12 h and then soaked in deionized water at 30 °C for one day.

$$\text{In-plane swelling } (\%) = \frac{A_{wet} - A_{dry}}{A_{dry}} \times 100 \quad (3)$$

$$\text{Through-plane swelling } (\%) = \frac{l_{wet} - l_{dry}}{l_{dry}} \times 100 \quad (4)$$

where A_{dry} and A_{wet} are the area of dried and wet membranes, respectively, while l_{dry} and l_{wet} are the thickness of dried and wet membranes, respectively.

The ion exchange capacity (IEC) of membranes was determined by acid–base titration. Membrane samples in the acid form were soaked in 1.0 M NaCl solution for one day, and then the solution was titrated with 0.01 M NaOH solution using phenolphthalein as an indicator. The IEC was calculated from the amount of NaOH consumed in the titration and the weight of the dried membrane samples. Volumetric IEC ($IEC_{v(dry)}$) was obtained by multiplying the IEC_w value and the membrane density. The $IEC_{v(wet)}$ was calculated based on water uptake measurements using the following equation.

$$IEC_{v(dry)} = IEC_w \times \text{density} \quad (5)$$

$$IEC_{v(wet)} = \frac{IEC_{v(dry)}}{1 + 0.01WU_v} \times 100 \quad (6)$$

The tensile strength and elongation of membranes were measured using a universal testing machine (Shimadzu, AGS-500NJ, Tokyo, Japan) following ISO37-4. Mechanical properties were measured under dry and wet conditions. Under wet conditions, samples were supplied with continuous humidification.

The proton conductivity of each membrane sample (size: 1 cm × 4 cm) was measured longitudinally under different RH conditions at 80 °C with a four-point probe alternating current (AC) impedance spectrometer (Solartron 1260, Farnborough Hampshire, ONR, UK). The measurements were performed in a thermo- and hydro-controlled chamber in an electronic noise-free environment. The proton conductivity (σ) was calculated from the following equation.

$$\sigma = \frac{L}{RS} \quad (7)$$

where L is the distance between the counter electrodes and the working electrode, R is the impedance of the membrane and S is the cross-sectional surface area of membrane samples (cm^2).

MEA fabrication and single cell performance

Membrane electrode assemblies (MEAs) were fabricated by the catalyst-coated substrate (CCS) method. Nafion perfluorinated ion-exchange resin solution (DuPont, USA) and 20 wt% Pt/C (Johnson Matthey Fuel Cell, USA) were mixed in water. The catalyst slurry was coated on gas diffusion layers (GDLs), both anode and cathode sides, until the weight of Pt loading reached 0.3 mg cm^{-2}. MEAs were fabricated by sandwiching the membranes between the anode and cathode electrodes and hot pressed at 130 °C under a pressure of 50 bar for 7 min. The prepared MEAs were tested in a single-cell fixture (with an active area of 5 cm^2). The PEFC tests were performed on single-cell test stations (WonATech, SMART I, Seoul, Korea). Electrochemical performances of cross-linked XESPSN membranes were measured under the following conditions. H_2 and O_2 were supplied at a flow rate of 100 cm^3 at 80 °C under 50% RH.

Results and discussion

The degree of sulfonation (DS) of ESPSN precursors was controlled to 50 to 70 mol%, corresponding to an IEC range of 1.96 to 2.49 meq. g^{-1}, and the number average molecular weights (M_n) were 18 to 30 kDa. The curing of ESPSN was conducted at

250 °C for 100 min in the solid membrane state *via* a thermally activated terminal ethynyl group trimerisation mechanism, without catalysts and initiators.[35–39] (Scheme 1).

Cross-linkable ESPSN structures were characterized by ^{1}H NMR. As shown in Fig. 1, the spectra show clear trends with changing DS. The signal intensities at 8.2 ppm (signal 1), 7.7 ppm (signal 2) and 6.9 ppm (signal 3) corresponding to the disulfonated group (SDCDPS) increased with the degree of sulfonation. On the other hand, the signal at 7.2 ppm (signal 6), corresponding to the DCBN moiety of the hydrophobic part decreased. The small signal at 4.2 ppm (signal 7) was assigned to the terminal ethynyl proton. ^{1}H NMR spectra confirmed the synthesized structure of the cross-linkable ESPSN.

DSC profiles of ESPSN60 are shown in Fig. 2a. As the scan time increased, T_g of ESPSN60 increased from 205 °C to 253 °C. In the first scan, a broad exothermic peak, which is derived from the curing reaction of the ethynyl moiety, was observed between 250 and 300 °C. However, the exothermic peak disappeared in the second and third scans, confirming the curing reaction was complete. Moreover to verify the degree of cross-linking at curing temperatures of ESPSN60, heat flow was observed by DSC isotherm experiments at 200 °C, 220 °C and 250 °C for up to 100 min (Fig. 2b). Exothermic heat flow was observed as the cross-linking reaction proceeded. Although the isothermal curing temperature was increased from 200 °C to 220 °C, both exothermic peaks at 200 °C and 220 °C exhibited very low intensities, less than 10 mW g^{-1}. However, at an isothermal curing temperature of 250 °C, more than 10 times higher increase in relative intensity of the exothermic peak was observed compared with that at 220 °C. About 80% of the thermal curing reaction took place within 20 min. After thermal curing for about 100 min, cross-linking was terminated. Therefore, 250 °C was selected as the optimal ethynyl end-group curing temperature of ESPSN.

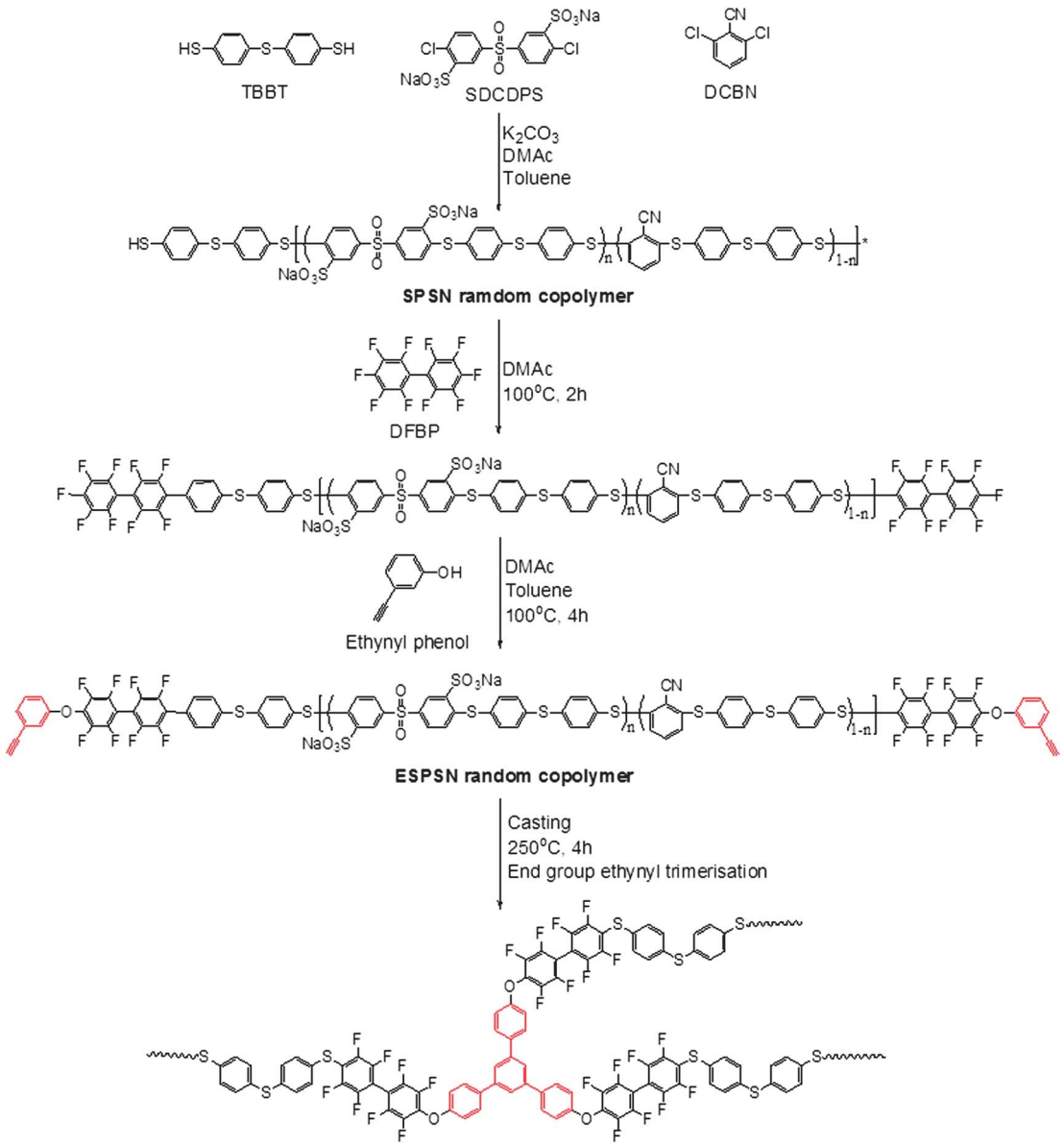

Scheme 1 Synthesis route of the polymer XESPSN.

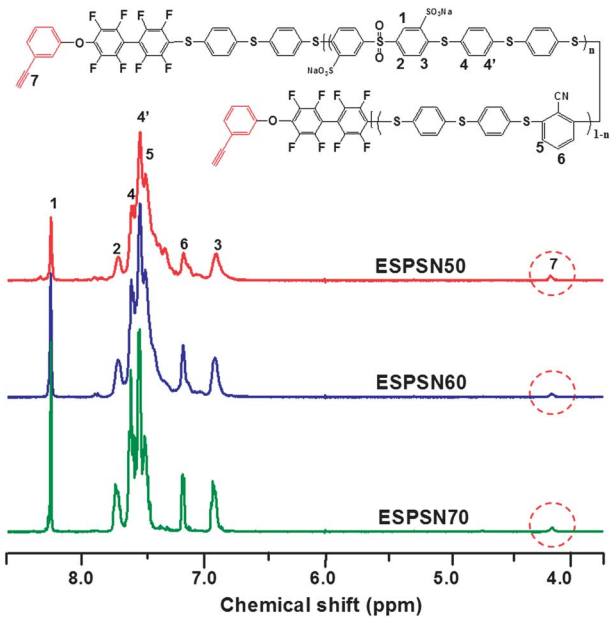

Fig. 1 ^{1}H NMR spectra of ESPSN.

After the thermal treatment, 3-D network formation was confirmed *via* solubility tests and gel-fraction measurements. At 30 °C, XESPSN membranes were insoluble in polar aprotic solvents such as DMAc and *N*-methylpyrrolidone (NMP), which are good solvents for the precursor ESPSN. The degree of cross-linking, based on the gel fraction, was over 97% (Table 1). Note that the mechanical properties of XESPSN were significantly improved when compared with those of ESPSN in the fully hydrated state. XESPSN exhibited mechanical toughness and stiffness comparable to Nafion® 212. In the dry state, the tensile strength of XESPSN was ~155% higher than that of ESPSN. However, elongation at break of XESPSN was about ~50% of ESPSSN. Improved tensile strength and reduction of elongation in the dry state of XESPSN is due to the presence of the cross-linking between polymer chains, which increases rigidity and strength of the polymer chains.

The cross-sectional nanophase-morphologies of ESPSN and XESPSN membranes (Fig. 3a–d) were obtained through transmission electron microscopy (TEM). The dark phase represents

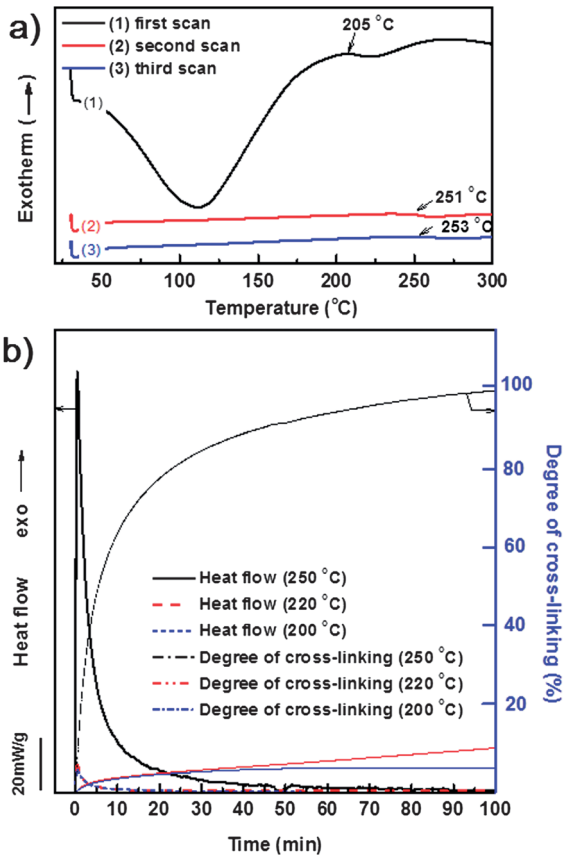

Fig. 2 (a) DSC curve of ESPSN60 and (b) degree of cross-linking of ESPSN60 with various thermal curing temperatures.

hydrophilic domains composed of sulfonate groups with lead counter cations. The hydrophilic domains in ESPSN are randomly distributed within the hydrophobic matrix, shown as the bright phase (Fig. 3a and S1†), with morphological features similar to many random copolymers having high IEC values; the size of the hydrophilic domains appears to be relatively large (>50 nm) and hydrophilic–hydrophobic phase separation is less developed. Surprisingly, thermally cured XESPSN copolymers exhibited well-defined, nanophase-separated morphologies (Fig. 3b–d) in spite of using amorphous random copolymer

Table 1 Molecular weight, mechanical strength and solubility of ESPSN and XESPSN copolymers

Copolymer	DS [mol%]	M_n[a] [kDa]	PDI[a]	Tensile strength[b] [MPa]		Elongation at break[b] [%]		Young's modulus[b] [MPa]		Solubility in DMAC	Gel fraction[c] [%]
				Dry	Wet	Dry	Wet	Dry	Wet		
ESPSN50	50	17.5	3.22	33.9 ± 8.7	17.1 ± 3.2	21.9 ± 2.3	22.0 ± 4.6	10	82	Yes	—
ESPSN60	60	29.5	2.77	44.5 ± 5.4	29.9 ± 3.9	31.4 ± 1.0	131.7 ± 13.2	21	129	Yes	—
ESPSN70	70	25.6	3.4	30.9 ± 5.4	13.9 ± 5.0	10.1 ± 0.4	103.8 ± 9.7	10	32	Yes	—
XESPSN50	50	—	—	46.9 ± 4.4	20.2 ± 0.4	10.0 ± 0.2	50.1 ± 16.9	11	251	Swollen	97.3
XESPSN60	60	—	—	59.9 ± 4.2	32.5 ± 1.2	15.2 ± 2.1	153.9 ± 15.3	25	380	Swollen	97.1
XESPSN70	70	—	—	69.0 ± 3.1	15.7 ± 1.1	13.7 ± 0.4	102.8 ± 7.40	13	117	Swollen	97.9
Nafion 212	—	—	—	22.5 ± 2.9	19.5 ± 0.3	200.4 ± 12.3	224.6 ± 10.6	2.3	50	—	—

[a] Determined by GPC using NMP with 0.05 M LiBr. [b] Measured at 30 °C. [c] Gel fraction was obtained from the ratio of the weight of the polymer after extraction from DMAc at 80 °C for 1 day and the initial weight.

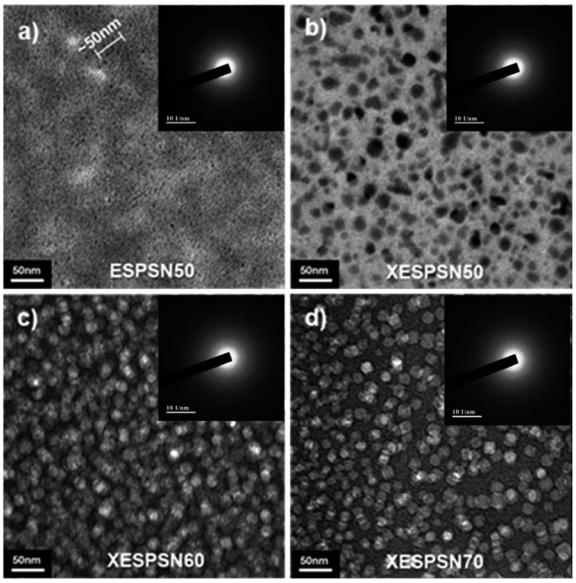

Fig. 3 TEM images and TEM-SAD patterns of the ESPSN50 precursor (a), XESPSN50 (b), XESPSN60 (c), and XESPSN70 (d).

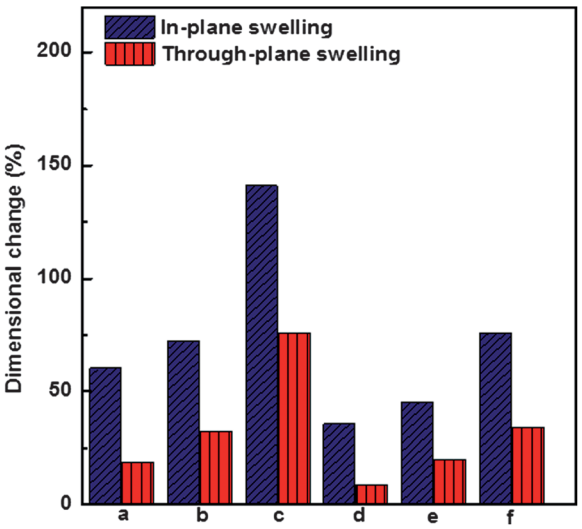

Fig. 4 Dimensional swelling of (a) ESPSN50, (b) ESPSN60, (c) ESPSN70, (d) XESPSN50, (e) XESPSN60, and (f) XESPSN70 in water at 30 °C.

precursors (Fig. S2†). Their morphological transformation is associated with thermally induced molecular rearrangement, where the driving force would be thermal annealing of ESPSN main chains,[41] in addition to thermal cross-linking of ethynyl terminal groups. Note that the glass transition temperatures (T_g) of ESPSN in the presence of residual DMAc ($T_g = 205$ °C) or in DMAc-free conditions ($T_g = \sim 253$ °C, Fig. 2a) are lower than or similar to the thermal curing temperature. During the thermal treatment at 250 °C, ESPSN undergoes thermal annealing leading to aggregation of both hydrophilic and hydrophobic moieties (see Fig. S3 and S4†).

The membrane morphological characteristics are highly dependent on their DS values. Relatively low DS XESPSN50 exhibits hydrophilic spheroidal clusters with non-uniform diameter size of 10–25 nm within interconnected hydrophobic copolymer phases (Fig. 3b), while XESPSN60 shows a worm-like morphology with a bi-continuous hydrophilic and hydrophobic network in narrow diameter ranges of 15–20 nm and 20–25 nm, respectively (Fig. 3c). For higher DS values of 60 to 70 mol%, the size of the interconnected hydrophilic domains increased up to 40 nm, while the hydrophobic domain size was somewhat reduced; Note that the morphological inversion between hydrophilic and hydrophobic phases became distinct as DS values increased. Furthermore small-angle X-ray scattering (SAXS) profiles of ESPSN50 and XESPSN membranes revealed that the inter-domain distance of ESPSN50 became wide from 4.48 to 6.28 nm after the thermal conversion into XESPSN50 (Fig. S5†). This behavior is of interest to us and needs further detailed studies in the future. These unusual and unique phase changes are expected to influence the proton transport behaviour through the XESPSN networks, particularly in a partially hydrated state.

Appropriate hydration of PEM materials is important in balancing proton conductivity and mechanical strength simultaneously. Linear copolymers with high DS values generally show high proton conductivity, but their excessive water swelling results in mechanical failures, particularly at interfaces with PEFC electrodes.[4] Excessively high water uptake dilutes the concentration of sulfonic acid groups per copolymer volume ($IEC_{v(wet)}$), which results in proton conductivity being lower than theoretical values.[40,41] This dilution effect on $IEC_{v(wet)}$ is obviously apparent in ESPSN70, since it has very high WU and λ values compared with ESPSN60, but lower $IEC_{v(wet)}$ (Table 2). Consequently, the proton conductivity and $IEC_{v(wet)}$ of

Table 2 Properties and stability of ESPSN and XESPSN membranes

Copolymer	Density[a] [g cm^{-3}]	IEC_w[b] [meq. g^{-1}]	$IEC_{v(dry)}$ [meq. cm^{-3}]	$IEC_{v(wet)}$ [meq. cm^{-3}]	WU[c] [%]	λ[d]	σ[e] [S cm^{-1}]	Oxidative stability[f] [wt%]	τ[g] [h]
ESPSN50	1.23	1.96	2.41	1.51	47.7	13.5	0.12	104.1	6.3
ESPSN60	1.25	2.20	2.75	1.53	64.1	16.2	0.16	NA[h]	NA[h]
ESPSN70	1.26	2.49	3.13	0.94	182.6	40.7	0.18	NA[h]	NA[h]
XESPSN50	1.23	2.02	2.48	1.81	29.8	8.2	0.15	111.6	7.3
XESPSN60	1.26	2.28	2.87	1.92	38.9	9.4	0.18	105.7	5.5
XESPSN70	1.28	2.53	3.23	1.15	140.5	30.8	0.20	104.3	3.5
Nafion 212	1.97	0.98	1.93	1.28	21.6	12.2	0.11	98.0	>50

[a] Measured from a known membrane dimension and weight after drying at 120 °C for 1 day. [b] Determined by titration. [c] Water uptake (WU) at 30 °C. [d] Hydration number = the mole ratios of H_2O to SO_3H. [e] Proton conductivity at 30 °C in water. [f] Residual weight percent of membranes after Fenton's test. [g] The time at which the membranes dissolved completely. [h] Not applicable: membrane formed hydrogel or dissolved.

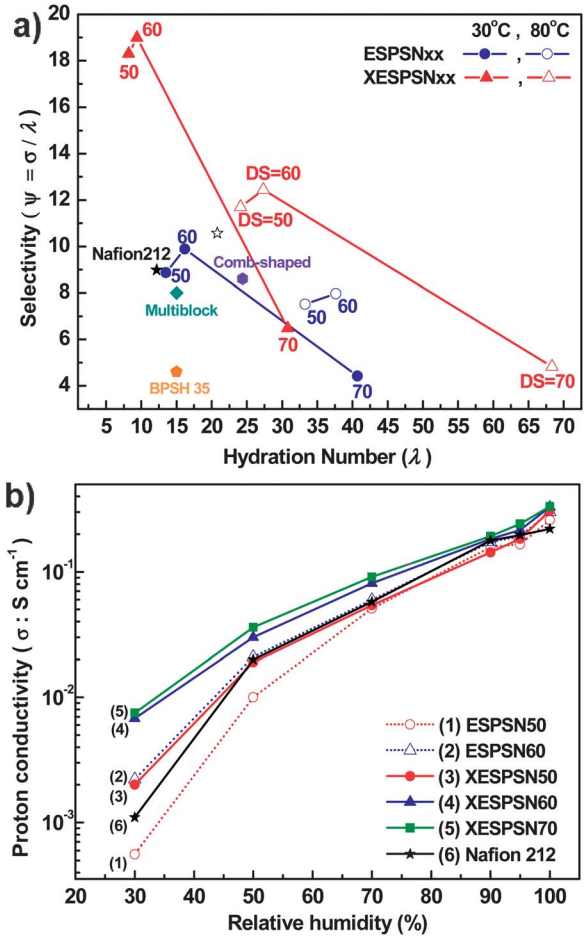

Fig. 5 (a) ψ for ESPSN, XESPSN membranes and Nafion® 212 at 30 °C and 80 °C in a fully hydrated state and (b) σ at different RH values and 80 °C.

ESPSN70 are lower than what would be expected in a linearly increasing conductivity trend. After cross-linking, membrane water uptake and water swelling ratios (Fig. 4) were reduced by ~48% and 25–38%, respectively, when compared to the corresponding ESPSN. The water uptake losses led to dramatically improved $IEC_{v(wet)}$ in the fully hydrated state (Table 2). Consequently, XESPSN exhibited proton conductivity superior to the corresponding ESPSN precursors and Nafion® 212, used as a reference. The rapid proton transport through XESPSN in water at 30 °C resulted from a synergetic effect of 3-D network formation-induced morphological transformation into well-defined hydrophilic–hydrophobic nanophase-separated domains and chain flexibility (as demonstrated by high elongation values in Table 1), in addition to its enhanced ionic concentration. The results also imply a high degree of connectivity within the proton-conducting hydrophilic phase.

Fig. 5a shows selectivity ($\psi = \sigma/\lambda$)[7] as a function of hydration number (λ) at 30 and 80 °C under fully hydrated conditions. The ψ values of XESPSN50 and 60 are higher than those of corresponding ESPSN PEMs and Nafion® 212. This implies that water molecules in XESPSN are more effectively utilized for proton transport as compared to other PEMs. For instance, XESPSN60 has ψ values higher than other highly phase-developed PEM materials including multiblock[7] and comb-shaped copolymers[10] at similar hydration levels. Interestingly, the favourable effect of 3-D network formation through end-group cross-linking on proton conduction was especially evident in partially hydrated states. Proton conductivities decreased with decreasing humidity, irrespective of which PEM materials were used (Fig. 5b). This reduction in proton transport capability with decreasing RH or dry states is typically observed and is associated with evaporation of proton carrier water molecules.[42] However, after 3-D network formation, the extent of proton conductivity reduction was largely alleviated in the measured RH range. Most significantly, the proton conductivity of XESPSN60 under RH 30% was 320% and 680% higher than those of ESPSN60 and Nafion® 212, respectively. The improved proton conduction observed in XESPSN is due to ordered nanophase morphology by high local density of sulfonic acid groups within the hydrophilic domain during cross-linking.

The oxidative stability, which indirectly shows PEM durability to free radical attack, was evaluated by comparing the PEM weight changes after soaking in Fenton's reagent (3 wt% H_2O_2 containing 2 ppm $FeSO_4$) at 80 °C for 1 h.[43] The time elapsed until complete membrane dissolution (τ) was also measured under the same conditions and is summarized in Table 2. All PEM materials except ESPSN60 and 70 showed modest weight gains as a result of oxidation from –S– to $–SO_2–$. ESPSN60 and 70 were dissolved in Fenton's reagent. However, the cross-linked counterparts XESPSN exhibited comparatively more stable oxidative resistance after the end-group curing, and thus were expected to show chemical resistance to PEM degradation under PEFC operation conditions.

Fig. 6 shows the current–voltage polarization curves of XESPSN60, ESPSN60, and Nafion® 212, which were obtained at 80 °C and 50% RH. All single cells were made using the same fabrication procedures and electrode composition in order to isolate the PEM contribution from PEFC performance.[44] XESPSN60 demonstrated the highest PEFC performance among the tested samples. At 0.6 V, its current density and maximum power density were ~160% and ~150% higher than those of ESPSN60 and Nafion® 212, respectively.

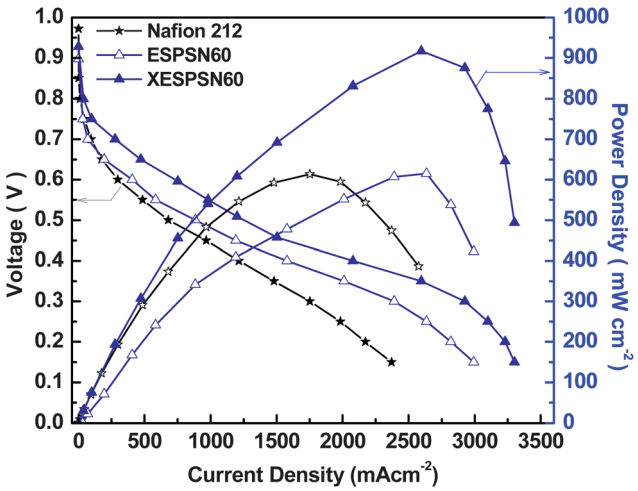

Fig. 6 H_2/O_2 PEFC performance of ESPSN60, XESPSN60 and Nafion® 212 at 80 °C with humidification at 50% RH.

Conclusions

In summary, a promising PEM material, XESPSN, was synthesized *via* polycondensation of SPSN copolymers with high DS values. The incorporated thermally curable ethynyl groups at the termini of the starting copolymers (ESPSN) led to 3-D network formation, resulting in unusual morphological transformation. XESPSN has well-developed hydrophilic–hydrophobic nanophase separation and high sulfonic acid density, and retains chain mobility for maintaining fast proton transport even in partially hydrated states. XESPSN showed outstanding low humidity PEFC performance when compared with other hydrocarbon PEM materials or Nafion® used in PEFCs.

Acknowledgements

This research was supported by the WCU (World Class University) program through the National Research Foundation of the Korean Ministry of Science and Technology (no. R31-2008-000-10092-0), and New & Renewable Energy R&D program (2008-N-FC12-J-01-2-100) under the Ministry of Knowledge Economy. We appreciate Prof. Thoman Thurn-Albrecht and Mr Tingzi Yan at Martin-Luther-Universitat, Germany for SAXS measurements.

Notes and references

1 C. E. Heath and A. G. Revfsz, *Science*, 1973, **180**, 542–544.
2 M. A. Hickner, H. Ghassemi, Y. S. Kim, B. R. Einsla and J. E. McGrath, *Chem. Rev.*, 2004, **104**, 4587–4612.
3 M. Rikukawa and K. Sanui, *Prog. Polym. Sci.*, 2000, **25**, 1463–1502.
4 C. H. Park, C. H. Lee, M. D. Guiver and Y. M. Lee, *Prog. Polym. Sci.*, 2011, **36**, 1443–1498.
5 K. B. Wiles, C. M. de Diego, J. de Abajo and J. E. McGrath, *J. Membr. Sci.*, 2007, **294**, 22–29.
6 H.-S. Lee, A. Roy, O. Lane, S. Dunn and J. E. McGrath, *Polymer*, 2008, **49**, 715–723.
7 A. Roy, X. Yu, S. Dunn and J. E. McGrath, *J. Membr. Sci.*, 2009, **327**, 118–124.
8 B. Bae, T. Yoda, K. Miyatake, H. Uchida and M. Watanabe, *Angew. Chem., Int. Ed.*, 2010, **49**, 317–320.
9 D. S. Kim, G. P. Robertson and M. D. Guiver, *Macromolecules*, 2008, **41**, 2126–2134.
10 N. Li, C. Wang, S. Y. Lee, C. H. Park, Y. M. Lee and M. D. Guiver, *Angew. Chem., Int. Ed.*, 2011, **50**, 9158–9161.
11 N. Li, S. Y. Lee, Y.-L. Liu, Y. M. Lee and M. D. Guiver, *Energy Environ. Sci.*, 2012, **5**, 5346–5355.
12 G. Dorenbos and K. Morohoshi, *Energy Environ. Sci.*, 2010, **3**, 1326–1338.
13 S. Matsumura, A. R. Hlil, C. Lepiller, J. Gaudet, D. Guay, Z. Shi, S. Holdcroft and A. S. Hay, *Macromolecules*, 2007, **41**, 281–284.
14 S. Matsumura, A. R. Hlil, N. Du, C. Lepiller, J. Gaudet, D. Guay, Z. Shi, S. Holdcroft and A. S. Hay, *J. Polym. Sci., Part A: Polym. Chem.*, 2008, **46**, 3860–3868.
15 C. Wang, N. Li, D. W. Shin, S. Y. Lee, N. R. Kang, Y. M. Lee and M. D. Guiver, *Macromolecules*, 2011, **44**, 7296–7306.
16 R. Devanathan, *Energy Environ. Sci.*, 2008, **1**, 101–119.
17 J. A. Kerres, *Fuel Cells*, 2005, **5**, 230–247.
18 A. M. Herring, *J. Macromol. Sci. Polymer Rev.*, 2006, **46**, 245–296.
19 K. Miyatake, T. Tombe, Y. Chikashige, H. Uchida and M. Watanabe, *Angew. Chem., Int. Ed.*, 2007, **46**, 6646–6649.
20 G. L. Athens, Y. Ein-Eli and B. F. Chmelka, *Adv. Mater.*, 2007, **19**, 2580–2587.
21 T. Yamaguchi, H. Zhou, S. Nakazawa and N. Hara, *Adv. Mater.*, 2007, **19**, 592–596.
22 J. B. Ballengee and P. N. Pintauro, *Macromolecules*, 2011, **44**, 7307–7314.
23 C. H. Lee, S. Y. Lee, Y. M. Lee, S. Y. Lee, J. W. Rhim, O. Lane and J. E. McGrath, *ACS Appl. Mater. Interfaces*, 2009, **1**, 1113–1121.
24 S. J. Lue, S.-Y. Hsiaw and T.-C. Wei, *J. Membr. Sci.*, 2007, **305**, 226–237.
25 Z. Bai, M. F. Durstock and T. D. Dang, *J. Membr. Sci.*, 2006, **281**, 508–516.
26 K. B. Wiles, F. Wang and J. E. McGrath, *J. Polym. Sci., Part A: Polym. Chem.*, 2005, **43**, 2964–2976.
27 Z. Bai, M. D. Houtz, P. A. Mirau and T. D. Dang, *Polymer*, 2007, **48**, 6598–6604.
28 H. Dai, H. M. Zhang, Q. T. Luo, Y. Zhang and C. Bi, *J. Power Sources*, 2008, **185**, 19–25.
29 J. K. Lee and J. Kerres, *J. Membr. Sci.*, 2007, **294**, 75–83.
30 M. Schuster, C. C. de Araujo, V. Atanasov, H. T. Andersen, K.-D. Kreuer and J. Maier, *Macromolecules*, 2009, **42**, 3129–3137.
31 M. Schuster, K.-D. Kreuer, H. T. Andersen and J. Maier, *Macromolecules*, 2007, **40**, 598–607.
32 D. S. Phu, C. H. Lee, C. H. Park, S. Y. Lee and Y. M. Lee, *Macromol. Rapid Commun.*, 2009, **30**, 64–68.
33 Y. S. Kim, D. S. Kim, B. Liu, M. D. Guiver and B. S. Pivovar, *J. Electrochem. Soc.*, 2008, **155**, B21–B26.
34 D. S. Kim, Y. S. Kim, M. D. Guiver and B. S. Pivovar, *J. Membr. Sci.*, 2008, **321**, 199–208.
35 K.-S. Lee and J.-S. Lee, *Chem. Mater.*, 2006, **18**, 4519–4525.
36 J.-P. Kim, W.-Y. Lee, J.-W. Kang, S.-K. Kwon, J.-J. Kim and J.-S. Lee, *Macromolecules*, 2001, **34**, 7817–7821.
37 M.-H. Jeong, K.-S. Lee and J.-S. Lee, *J. Membr. Sci.*, 2009, **337**, 145–152.
38 K.-S. Lee, M.-H. Jeong, J.-P. Lee and J.-S. Lee, *Macromolecules*, 2009, **42**, 584–590.
39 M.-H. Jeong, K.-S. Lee and J.-S. Lee, *Macromolecules*, 2009, **42**, 1652–1658.
40 Y. S. Kim and B. S. Pivovar, *Annu. Rev. Chem. Biomol. Eng.*, 2010, **1**, 123–148.
41 C. H. Lee, K.-S. Lee, O. Lane, J. E. McGrath, Y. Chen, S. Wi, S. Y. Lee and Y. M. Lee, *RSC Adv.*, 2012, **2**, 1025–1032.
42 K.-D. Kreuer, *Chem. Mater.*, 1996, **8**, 610–641.
43 N. Asano, M. Aoki, S. Suzuki, K. Miyatake, H. Uchida and M. Watanabe, *J. Am. Chem. Soc.*, 2006, **128**, 1762–1769.
44 D. S. Hwang, C. H. Park, S. C. Yi and Y. M. Lee, *Int. J. Hydrogen Energy*, 2011, **36**, 9876–9885.

